

Study on 3-D Flow Patterns in Yarn Channels of an Interlacer

College of Textile and Clothing,
Jiangnan University,
Wuxi, 214000, China
E-mail: qiu_hua@jiangnan.edu.cn

Abstract

The aim of the present work was to determine the flow characteristics of compressible airflow in the yarn channel of an interlacer by numerical simulations to make clear the effects of cross-sectional shapes of the yarn channel on the performance of interlacers. CFD (Computational Fluid Dynamics) software package ANSYS CFX was used to calculate flow patterns in the yarn channel. Relations between the performance of the interlacer and distribution of the velocity vector, airflow speed and particle trace of the flow were clarified to provide knowledge to design better interlacers.

Key words: interlacer, flow patterns, computational fluid dynamics, performance.

Introduction

Du Pont invented interlacing technology in 1961 [1]. It can be used to improve the cohesion between multi-filament yarn, to facilitate winding-up and unwinding and to produce novel yarn [2].

The interlacing device, known as an interlacer, plays an important role in the interlacing process. A simple interlacer

is composed of an air jet nozzle, yarn channel and two yarn guides. By blowing compressed air on a yarn running through the yarn channel, filaments tangle with each other to form interlaced yarn with alternate tangling and opening parts. The interlacer is the key part in the interlacing process. Yarn interlacing is the result of compressed air acting on a bundle of loose filaments; hence the airflow patterns strongly affect the characteristics of interlaced yarn and the performance of the interlacer. Many works have been carried out to make clear some airflow patterns, such as static pressure on the yarn channel [4, 5] and dynamic pressure near it [6], either by an experimental method [4 - 6], computation method [7] or by a combination of these two methods [8, 9]. Most of these papers paid much attention to the measurement of airflow patterns. However, little attention was paid to the relation between the performance of the interlacer and flow patterns. On the other hand the traditional way of designing new types of interlacer

needs its manufacture and many experiments afterwards, which is time consuming and expensive.

In a previous research, seven interlacers with various cross-sectional shapes of the yarn channel were made and then the effect of various cross-sectional shapes of the yarn channel on characteristics of the interlaced yarn [10] and yarn motion in the yarn channel [11] were clarified. Cross-sectional shapes and sizes of yarn channels are shown in **Figure 1**. The diameter of the air jet nozzle is 1.4 mm, and the distance between two yarn guides - 25.4 mm. Notation C1 represents the interlacer with a circular cross-sectional yarn channel. E1, E2 and E3 are interlacers with an elliptical yarn channel. S1 has a square yarn channel, and T1 and T2 have a triangular one.

On the basis of previous research [12] which aimed to find an effective way to simulate airflow in the yarn channel, we

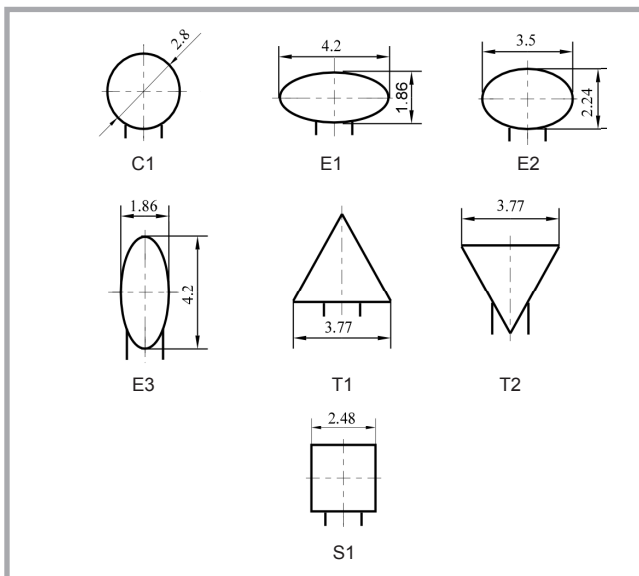


Figure 1. Cross-sectional shapes and sizes of yarn channels (Unit: mm).

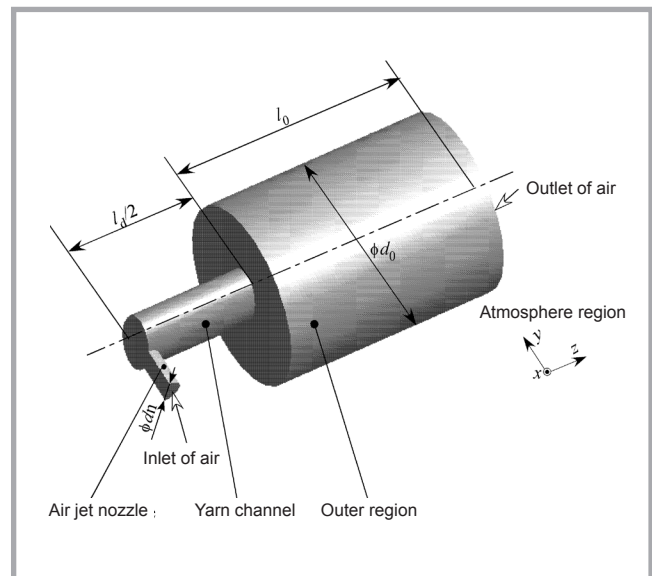


Figure 2. Geometry used in simulation.

Table 1. Sizes of the outer region.

Interlacer	Size of the outer region	
	d_0 , mm	l_0 , mm
C1	14.00	56.00
E1	21.00	84.00
E2	17.50	70.00
E3	21.00	84.00
T1	21.77	87.08
T2	21.77	87.08
S1	17.54	70.16

Table 2. Computation conditions at the entrance of air jet nozzle.

p_0 , MPa (Gauge pressure)	p_{in} , MPa (Absolute pressure)	T_{in} , K	v_{in} , m/s
0.2	0.159	244.1	313.1
0.3	0.212		
0.5	0.317		

calculated flow patterns in these seven interlacers with a commercial CFD software package - ANSYS CFX. The aim of the present work is to clarify the relations between the performances of interlacers and flow patterns in the yarn channel and to provide knowledge for the better design of interlacers.

Simulation

Geometry

Figure 2 shows the geometry used in simulation (taking interlacer E2 as an example). Each geometry was composed of three parts: an air jet nozzle, yarn channel and outer region. The diameter d_0 and length l_0 of the outer region were five times and twenty times that of the diameter of the yarn channel, respectively. Half of the interlacer origin was used because of the symmetry to save the time of calculation. Table 1 gives the sizes of each outer region.

Boundary conditions

Since these seven interlacers can produce interlaced yarn with a large number of tangles at supplied air pressure $p_0 = 0.3$ MPa (gauge pressure) [10], flow patterns in the yarn channel at that pressure were simulated. Moreover because interlacers E2 and T2 outperform the other interlacers, flow patterns in their yarn channels at $p_0 = 0.2$ and 0.5 MPa were simulated.

A compressed air reservoir supplied compressed air for yarn interlacing. In the air reservoir, p_0 is adjustable, temperature $T_0 = 293$ K and flow speed $v_0 = 0$ m/s. The atmospheric pressure

is $p_b = 0.1013$ MPa (absolute pressure), temperature $T_b = 293$ K and speed $v_b = 0$ m/s. When p_0 is 0.2 MPa, because $p_b/(p_b + 0.1013)$ is less than 0.528 , air chokes in the air jet nozzle and the speed of the air v_{in} at the entrance of the air jet nozzle is equal to that of the sound, which is decided by the temperature at the entrance of the air jet nozzle T_{in} [13]. Table 2 gives computation conditions at the entrance of the air jet nozzle.

The airflow in the yarn channel is turbulent and hence the standard $k - \epsilon$ model of turbulent fluid is used. Compressed air in the interlacer is taken as viscous and compressible ideal gas. Yarn is neglected in simulation because its volume is low compared with the high pressure and velocity of the compressed air.

Since the yarn channel is very short and the speed of compressed air is very high, the interlacing process is completed in a very short time. For simplification, we assumed that the process is adiabatic, i.e. no heat transfers through the wall of the interlacer. On the wall of the yarn channel and air jet nozzle, no slip is applied. Figure 3 shows the positions of the boundary condition geometrically.

Mesh generation

The numerical method used for discretisation in CFX was the finite volume method (FVM). This approach involves subdividing the entire flow geometry into finite control volumes using a mesh [14].

ANSYS ICEM was used to generate an unstructured triangular mesh. Figure 3.a shows the shape of the mesh element. Figure 3.b indicates the distribution of

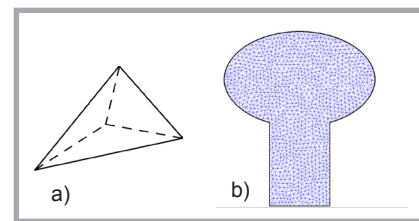


Figure 3. Mesh in simulation; a) shape of mesh element, b) distribution of mesh elements on plane $z = 0$ mm in interlacer E2.

mesh elements on plane $z = 0$ mm, the cross-section of the yarn channel including the axis of the air jet nozzle, in interlacer E2.

Computational scheme and computer

The numerical technique utilised for discretisation was the upwind difference scheme (UDS).

Iteration of the computation is set to 1000, which can ensure the calculation stops because the RMS (residual of root mean square) $= 1 \times 10^{-5}$ is satisfied. The computer used for calculation has two CPUs (2.2 GHz, AMD Opteron) and 12G RAM.

Results and discussion

Performance of seven interlacers

The performance of an interlacer is evaluated from the characteristics of the interlaced yarn it produces. A better interlacer can produce interlaced yarn with a large N , number of tangling parts per meter, and proper S , strength of tangling parts [10].

Figure 4 shows a comparison of the performance of seven interlacers at supplied air pressure $p_0 = 0.3$ MPa, yarn speed $v = 200$ m/min and overfeed ratio $F = 2\%$.

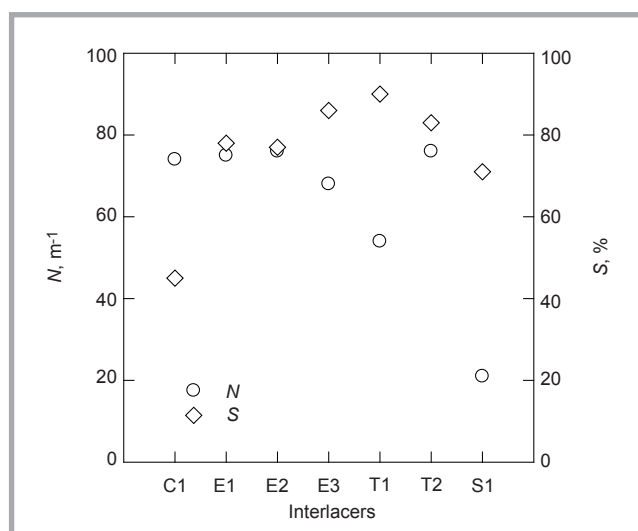


Figure 4. Comparison of the performance of seven interlacers at supplied air pressure $p_0 = 0.3$ MPa, yarn speed $v = 200$ m/min and overfeed ratio $F = 2\%$.

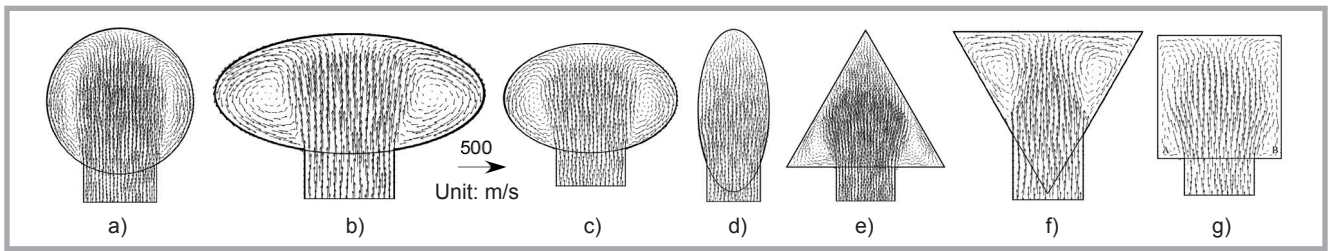


Figure 5. Distribution of velocity vectors on plane $z = 0$ mm in seven interlacers at $p_0 = 0.3$ MPa; a) C1, b) E1, c) E2, d) E3, e) T1, f) T2, g) S1.

$v = 200$ m/min and overfeed ratio $F = 2\%$.

Among them, the round yarn channel is good for yarn interlacing and the cornered yarn channel can produce an interlaced yarn with higher strength of tangles.

Distribution of air velocity vectors on plane $z = 0$ mm

The yarn on plane $z = 0$ mm was acted upon by compressed air directly from the air jet nozzle. Yarn motion on plane $z = 0$ mm characterised the yarn interlacing. Since the yarn was light, flow patterns on plane $z = 0$ mm greatly affected yarn motion.

Figure 5 shows the distribution of velocity vectors on plane $z = 0$ mm in seven interlacers at $p_0 = 0.3$ MPa. Before the interlacing process, the yarn position was along half of the height of the

yarn channel and intersected the axis of the air jet nozzle. Flow patterns on the cross-section of yarn channel including the axis of air jet nozzle decide both the yarn motion and the space for interlacing yarn.

From **Figure 5**, except for interlacer E3, symmetric vortexes occur on plane $z = 0$ mm in the other six interlacers. In interlacer E3, since the width of the yarn channel is close to the diameter of the air jet nozzle, no obvious vortexes appear. Yarn is difficult to run to the lower part of the yarn channel and cannot be interlaced sufficiently in E3 because reverse flows on plane $z = 0$ mm are weak.

In interlacer S1, vortexes occur at corners A and B, where the speed of flow is lower. Yarn is easy to be trapped in corners for a long time because of the lower speed flow. Hence interlacer S1 has poor performance.

In interlacer T1, vortexes at the bottom of the yarn channel have little effect on yarn motion because the high speed flow blows yarn to the upper part of the interlacer. As for interlacer T2, since the top two corners are beyond the two vortexes, the corners slightly influence yarn motion.

In interlacer E3, the effect of two vortexes on yarn motion is something like that of S1. In its yarn channel, yarn stays in the vortexes for a long time.

Vortexes on plane $z = 0$ mm in interlacers C1 and E2 can afford a big space for yarn interlacing and they can produce interlaced yarn with a large number of tangles.

Contour of air speed U_y on plane $z = 0$ mm

We know that opening yarn by compressed air is essential to yarn interlacing. Since the opening of yarn is performed by the action of compressed air, it was strongly affected by U_y , the velocity of the flow in the y -direction.

Figure 6 shows the contour of U_y on plane $z = 0$ mm in interlacers C1, E1, E2, E3, T1 and T2 ($p_0 = 0.3$ MPa). We omitted interlacer S1 because it has the poorest performance. From **Figure 6**, the highest flow speeds, which decide the opening of yarn, are at the center of the cross-section of the yarn channel. **Figure 7** shows U_y at the intersection (origin) of the initial yarn position and the axis of the air jet nozzle in interlacers C1, E1, E2, E3, T1 and T2 ($p_0 = 0.3$ MPa). Among these six interlacers, U_{y0} & U_y at the origin in interlacers C1, E2 and T2 are higher and close to each other. In interlacers E1, E3 and T1, U_{y0} are lower, especially in T1. In this case, yarn cannot be opened sufficiently. Moreover in interlacer E3, as shown in **Figure 6.d**, the distribution of higher speed flows prevent yarn from running to the low part of the

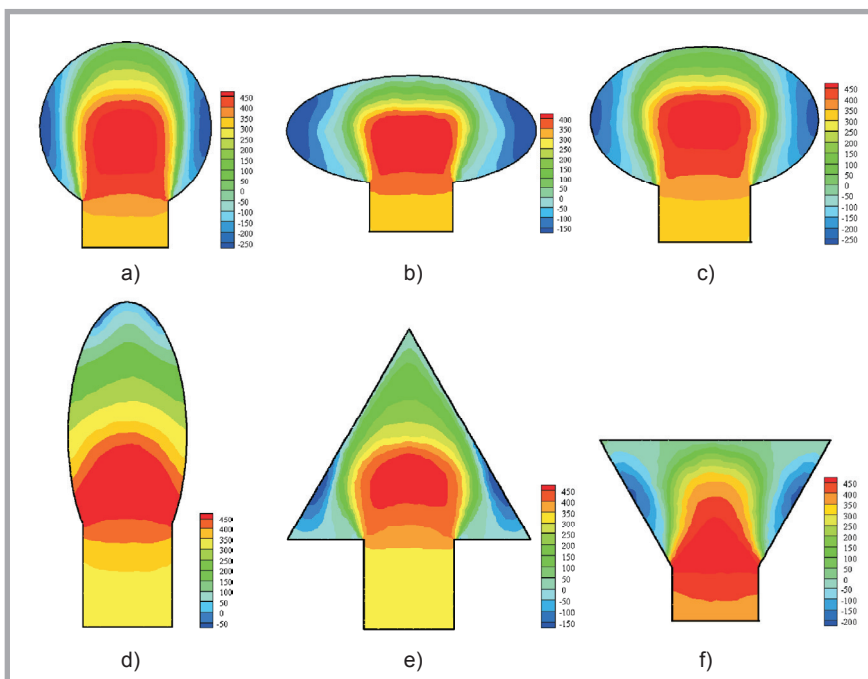


Figure 6. Contour of U_y on plane $z = 0$ mm in interlacers C1, E1, E2, E3, T1 and T2 ($p_0 = 0.3$ MPa); a) C1, b) E1, c) E2, d) E3, e) T1, f) T2 (Unit: m/s).

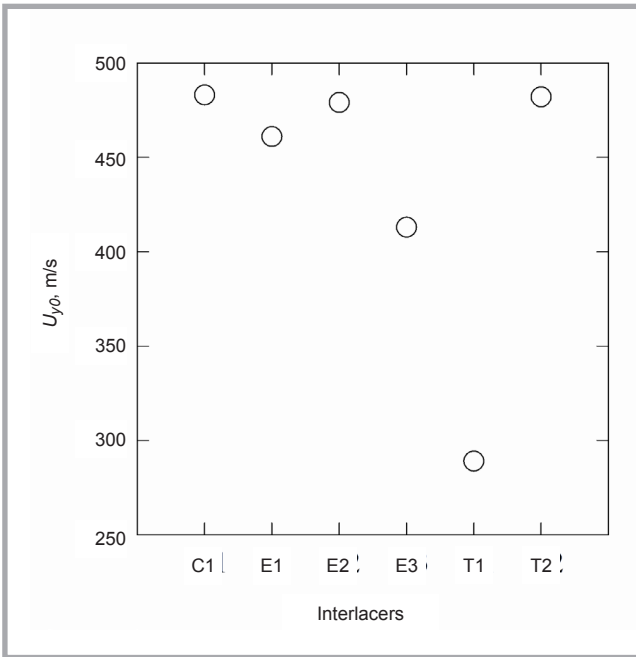


Figure 7. U_y at the intersection (origin) of the initial yarn position and the axis of the air jet nozzle in interlacers C1, E1, E2, E3, T1 and T2 ($p_0 = 0.3$ MPa)

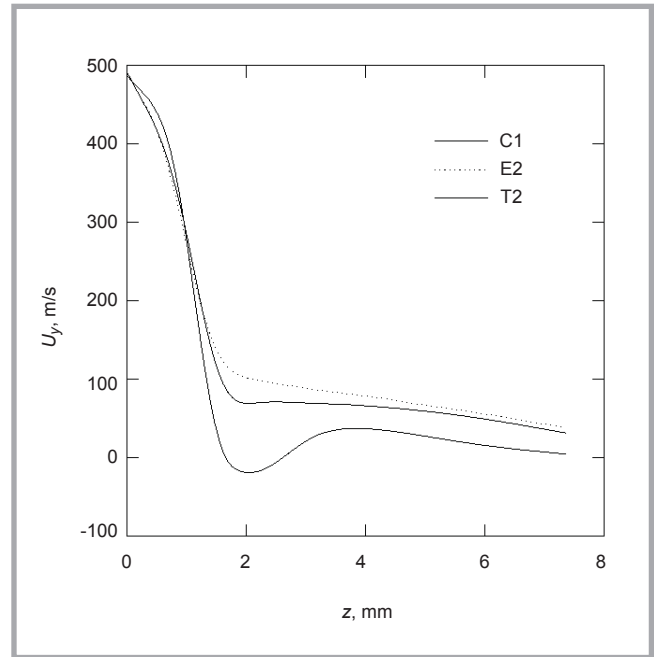


Figure 8. Distribution of U_y at the initial yarn position in interlacers C1, E2 and T2.

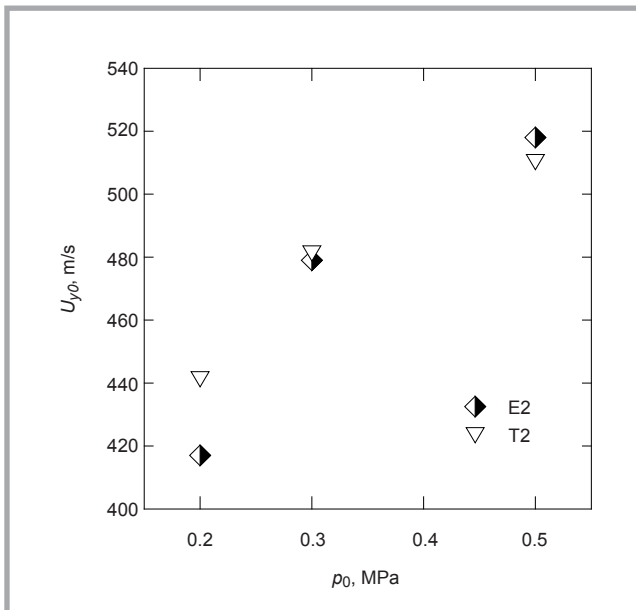


Figure 9. Relation between U_{y0} and supplied air pressure p_0 in interlacers E2 and T2.

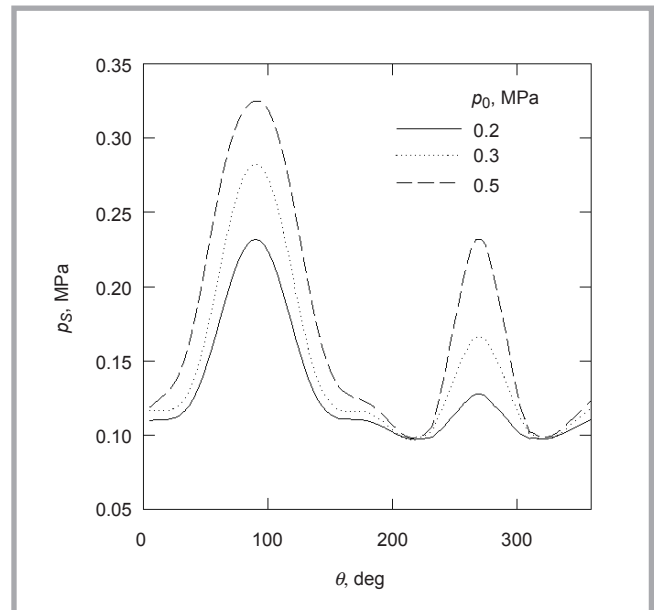


Figure 10. Distribution of static pressure p_s (absolute pressure) on the circumference of E2 at various p_0 ($z = 0$ mm).

yarn channel, hence yarn is interlaced in a small space. For interlacer E1, because of the wider yarn channel, compressed air expands after entering the yarn channel and the flows cannot have higher speed, which is not good for opening yarn.

Air speed U_y at initial yarn position

Figure 8 shows the distribution of U_y at the initial yarn position in interlacers C1, E2 and T2. We chose them because they can open the yarn at the origin position well. As shown in the Figure, U_y

decreases sharply in region $z = 0 - 2$ mm, and then to 0 m/s, which means that the yarn is mainly opened in the middle part of the yarn channel. Designing interlacers with higher U_y at the initial yarn position is important to improve the number of tangles.

Flow patterns in interlacers E2 and T2

Interlacers E2 and T2 outperform the others when both the number and strength of tangles are considered. They can produce interlaced yarn with larger N at sup-

plied pressure $p_0 = 0.3$ MPa, not at 0.2 nor 0.5 MPa.

Figure 9 shows the relation between U_{y0} and supplied air pressure p_0 in interlacers E2 and T2, indicating that U_{y0} increases with p_0 and the U_{y0} in interlacers E2 and T2 is close when $p_0 > 0.3$ MPa. Since the opening of the yarn is improved, the number of tangles also increases. However, in a previous study [10], the interlacer produced interlaced yarn with a smaller number of tangles at $p_0 = 0.5$ MPa.

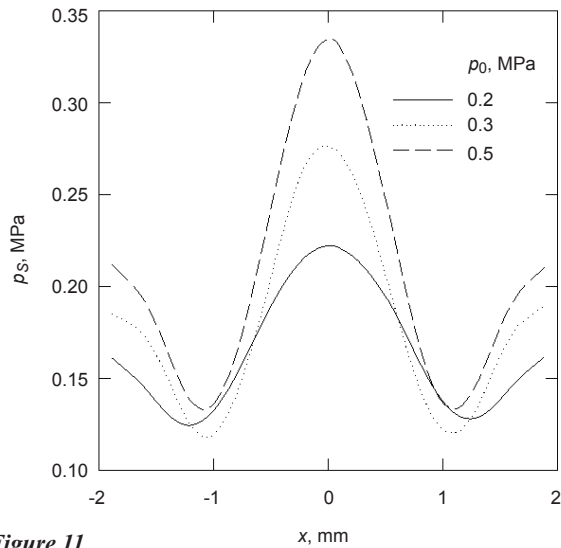


Figure 11.

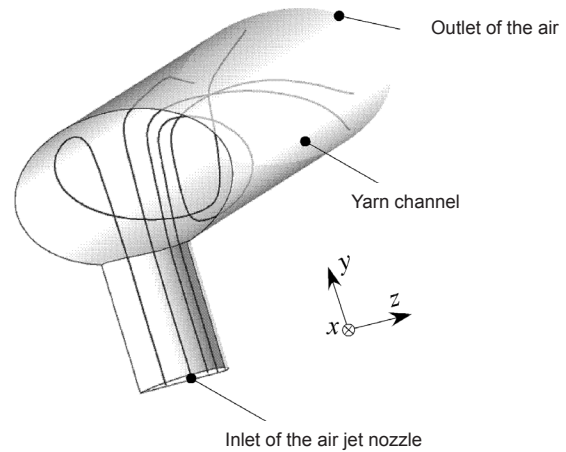


Figure 12.

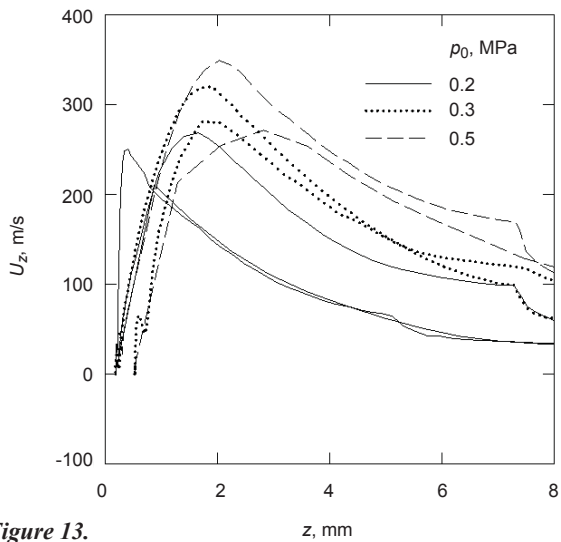


Figure 13.

Figure 11. Distribution of static p_s at the top of the yarn channel in interlacer T2 at various p_0 ($z = 0$ mm).

Figure 12. Particle trace of flow starting from the inlet of the air jet nozzle in interlacer E2.

Figure 13. Distribution of U_z on particle trace of flow at various supplied air pressures p_0 .

Figure 10 shows the distribution of static pressure p_s (absolute pressure) on the circumference of E2 at various p_0 ($z = 0$ mm). Figure 11 shows the distribution of static p_s at the top of the yarn channel in interlacer T2 at various p_0 ($z = 0$ mm). From the figures, p_s increases with p_0 and reaches the maximum at the extension of the axis of the air jet nozzle. Yarn is easy to stay in the yarn channel when $p_s > 0.28$ MPa and the continuous yarn motion is interrupted.

U_z on particle trace of the flow

Yarn motion in the yarn channel is decided by flow patterns because the speed of flow is high and the yarn light. In a previous paper [15], it was difficult to observe three dimensional yarn motions in the yarn channel by eye or stroboscope. By visualising the results of CFD, we can observe the particle trace of flow in the

yarn channel clearly. Figure 12 shows the particle trace of flow starting from the inlet of the air jet nozzle in interlacer E2. The trace of the flow particle is a forwarding helix running against the wall of the yarn channel.

Figure 13 shows the distribution of U_z on the particle trace of flow at various supplied air pressures p_0 . U_z is the velocity of the flow in the z -direction along the axis of the yarn channel, which affects the tension of yarn in interlacing, which is like that of the overfeed ratio on yarn interlacing. From the figure, U_z increases first, reaches the maximum at $z = 2$ mm, and then decreases. When the air pressure supplied increases from 0.2 to 0.5 MPa, U_z decreases in the region $z = 0$ to 2 mm. In this case, yarn tension also decreases, which makes the yarn open easily. When $p_s = 0.2$ MPa, because U_z is

large, yarn tension is higher, which prevents the opening of yarn.

Conclusions

In this study, flow patterns in seven interlacers with various cross-sectional shapes of yarn channels were computed using the CFD software package ANSYS CFX. The performance of the interlacer was decided by flow patterns in its yarn channel.

- 1) Vortexes at plane $z = 0$ mm affect the space for yarn interlacing.
- 2) The velocity of the flow affects yarn interlacing in two aspects: U_y , air velocity along the axis of the air jet nozzle affects the yarn opening, and U_x , air velocity along the axis of the yarn channel affects yarn tension. Higher

U_y and lower U_x are good for the opening of yarn.

- Higher supplied air pressure is good for yarn opening. However, too high supplied air pressure will blow and hold yarn on the yarn channel wall for a long time, which decreases the number of tangles.
- The trace of flow particle in the yarn channel is helical.
- The opening and tangling of yarn proceed mainly in the middle part of the interlacer.



Acknowledgements

The authors are grateful for financial support from Fundamental Research Funds for the Central Universities (No. JUSRP51301A)

References

- Iemoto Y, Tanoue S. An Introchannelion to Computational Fluid Dynamics-The Finite Volume Method (Ed. 2008). Longman, New York, 1995, pp. 49-53
- Negishi T, Kojima T. Japanese Open Official Gazette of Patents, Showa 57-71427 (In Japanese), 1982.
- Iemoto Y. *Japanese Journal of Multiphase Flow* 1997; 11, 1: 23-29.
- Iemoto Y, Chono S. *J. Text. Mach. Soc. Japan*. 1997; 43: 38-46.
- Iemoto Y, Chono S, Qin H. *J. Text. Eng.* 2000; 46: 11-19.
- Iemoto Y, Tanoue S, Lu J. *J. Text. Eng.* 2009; 55, 111-118.
- Rengasamy RS, Kothari VK, Patnaik A, Punekar H. *J. Text. Inst.* 2006; 97: 89-96.
- Murakami K, Tokunaga K, Nomura S, Naito S, Abe M. *J. Text. Eng.* 2006; 52: 73-79.
- Tokunaga K, Murakami K, Kitamura M, Nomura S. *J. Text. Eng.* 2006; 52: 121-129.
- Qiu H, Iemoto Yoshiyuki, Tanoue Shuichi. *J. Text. Eng.* 2007; 53: 1-8.
- Qiu H, Iemoto Y, Tanoue S. *J. Text. Eng.* 2007; 53: 59-67.
- Qiu H, Iemoto Y, Tanoue S. *J. Text. Eng.* 2010; 56: 87-96.
- Anderson JD. *Modern Compressible Flow*. McGraw-Hill Inc., 1990: 60.
- ANSYS Europe Ltd. 2005. ANSYS CFX-solver, Release 10.0: Theory: 26.
- Demir A. *Textile Asia* 1990; 13: 114-122.

Received 20.09.2012 Reviewed 02.07.2013



INSTITUTE OF BIOPOLYMERS AND CHEMICAL FIBRES

LABORATORY OF PAPER QUALITY

Since 02.07.1996 the Laboratory has had the accreditation certificate of the Polish Centre for Accreditation No AB 065.



The accreditation includes tests of more than 70 properties and factors carried out for:

- pulps
- tissue, paper & board,
- cores,
- transport packaging,
- auxiliary agents, waste, wastewater and process water in the pulp and paper industry.

The Laboratory offers services within the scope of testing the following: raw materials, intermediate and final paper products, as well as training activities.

Properties tested:

- general (dimensions, squareness, grammage, thickness, fibre furnish analysis, etc.),
- chemical (pH, ash content, formaldehyde, metals, kappa number, etc.),
- surface (smoothness, roughness, degree of dusting, sizing and picking of a surface),
- absorption, permeability (air permeability, grease permeability, water absorption, oil absorption) and deformation,
- optical (brightness ISO, whiteness CIE, opacity, colour),
- tensile, bursting, tearing, and bending strength, etc.,
- compression strength of corrugated containers, vertical impact testing by dropping, horizontal impact testing, vibration testing, testing corrugated containers for signs „B” and „UN”.

The equipment consists:

- micrometers (thickness), tensile testing machines (Alwetron), Mullens (bursting strength), Elmendorf (tearing resistance), Bekk, Bendtsen, PPS (smoothness/roughness), Gurley, Bendtsen, Schopper (air permeance), Cobb (water absorptiveness), etc.,
- crush tester (RCT, CMT, CCT, ECT, FCT), SCT, Taber and Lorentzen&Wettre (bending 2-point method) Lorentzen&Wettre (bending 4-point method and stiffness resonance method), Scott-Bond (internal bond strength), etc.,
- IGT (printing properties) and L&W Elrepho (optical properties), etc.,
- power-driven press, fall apparatus, incline plane tester, vibration table (specialized equipment for testing strength transport packages),
- atomic absorption spectrometer for the determination of trace element content, pH-meter, spectrophotometer UV-Vis.

Contact:

INSTITUTE OF BIOPOLYMERS AND CHEMICAL FIBRES
ul. M. Skłodowskiej-Curie 19/27, 90-570 Łódź, Poland
Elżbieta Baranek Dr eng. mech.,
tel. (+48 42) 638 03 31, e-mail: elabarane@ibwch.lodz.pl